

Comparative proteomics identify HSP90A, STIP1 and TAGLN-2 in serum extracellular vesicles as potential circulating biomarkers for human adenomyosis

DAYONG CHEN^{1,2}, LING ZHOU¹, HAI QIAO¹, YITING WANG¹, YAO XIAO¹,
LIAOQIONG FANG¹, BING YANG² and ZHIBIAO WANG¹

¹State Key Laboratory of Ultrasound in Medicine and Engineering, College of Biomedical Engineering, Chongqing Medical University, Chongqing 400016; ²Department of Obstetrics and Gynecology, The Affiliated Hospital of Zunyi Medical University, Zunyi, Guizhou 563000, P.R. China

Received November 25, 2020; Accepted December 22, 2021

DOI: 10.3892/etm.2022.11301

Abstract. Extracellular vesicles (EVs) carry specific proteins involved in intercellular communication. EVs with different protein contents are released into circulation in different diseases. Recent studies have identified proteins in adenomyosis (AM)-derived EVs (AMEVs) from blood as biomarkers for this disease. AM is an extension of endometrial tissue into the uterine myometrium. Magnetic resonance imaging (MRI) is the most accurate imaging tool for identifying adenomyosis. Therefore, the present study aimed to investigate the role of EVs in diagnosing AM. In the present study, tissue AMEVs (T-AMEVs) were isolated from lesion homogenates of patients with adenomyosis, and blood AMEVs (B-AMEVs) were isolated from peripheral blood of patients with AM via differential centrifugation and density gradient centrifugation. T-AMEVs and B-AMEVs were characterized by electron microscopy, western blotting and mass spectrometry and analysed using FunRich3.1.3 software. T-AMEVs (average diameter, 150.9±102.2 nm) and B-AMEVs (194.1±66.81 nm) expressed the CD9, CD63 and flotillin-2 EV markers. A total of 211 proteins expressed in T-AMEVs and B-AMEVs overlapped with Vesiclepedia database entries, including 2 epithelial-to-mesenchymal transition (EMT)-associated

proteins and 6 invasion-associated proteins. Gene Ontology and Kyoto Encyclopedia of Genes and Genomes (KEGG) pathway analysis indicated that these 211 proteins were associated with the ‘regulation of cell morphogenesis’ and ‘cytoskeletal organization’ terms, as well as the PPAR and HIF-1 signalling pathways, which are related to the proliferation and metastasis of endometrial cells that cannot invade the myometrium under normal circumstances. Among the 211 proteins, HSP90A, STIP1 and TAGLN-2 were expressed in T-AMEVs and B-AMEVs, but not in serum EVs of women without adenomyosis/endometriosis, and these proteins might be the potential biomarkers for adenomyosis. These findings provide insights into the molecular features of adenomyosis and the new candidate biomarkers for diagnosis.

Introduction

Adenomyosis is characterized as the abnormal ingrowth and invagination of the basal endometrium into the myometrium. Previous studies have documented an incidence rate of 30-50% (1). However, in infertile women with endometriosis, the incidence rate of adenomyosis increases to 70% (1). Therefore, the detection of adenomyosis in patients with infertility is important.

Extracellular vesicles (EVs) are secreted by most cells and can be transported; they can exchange cargo between cells as a means of intercellular communication at both the paracrine and systemic levels (2). EVs can travel systemically and target cells at very distant sites (3). EVs represent an information carrier for the originating cell and transport a variety of molecules, such as nucleic acids, cytokines, membrane-bound receptors and other biologically active lipids and proteins (4). EV composition is largely determined by the cell type and the physiological or pathological conditions of the producing cell (5). Moreover, the contents of EVs also reflect cell-specific pathological processes with membrane protection, and EVs have great potential to serve as circulating biomarkers that might improve current cancer diagnosis (6). Recent research suggests that EVs derived from adenomyosis endow endometrial epithelial cells with an invasive phenotype via

Correspondence to: Professor Bing Yang, Department of Obstetrics and Gynecology, The Affiliated Hospital of Zunyi Medical University, 143 Dalian Road, Zunyi, Guizhou 563000, P.R. China

E-mail: yangbing2188@163.com

Professor Zhibiao Wang, State Key Laboratory of Ultrasound in Medicine and Engineering, College of Biomedical Engineering, Chongqing Medical University, 1 Yixueyuan Road, Yuzhong, Chongqing 400016, P.R. China

E-mail: wangzb@cqmu.edu.cn

Key words: adenomyosis, extracellular vesicle, mass spectrometry, biomarker, proteome

epithelial-to-mesenchymal transition (EMT) (7). Therefore, adenomyosis-derived EVs (AMEVs) may carry specific proteins that reveal the pathological status of adenomyosis. Establishing these proteins as biological biomarkers is thus pivotal for the early diagnosis of adenomyosis.

A previous study confirmed that EVs exist in the plasma of patients with endometriosis (8), and tissue-derived AMEVs (T-AMEVs) have been isolated from adenomyosis lesion homogenates and blood-derived AMEVs (B-AMEVs) from the peripheral blood of patients with adenomyosis (7). Liquid chromatography-mass spectrometry (LC-MS) has been used to assess the proteins characteristics of T-AMEVs and B-AMEVs to more accurately identify functional proteins and molecular biomarkers in EVs for adenomyosis diagnosis (7). The present study aimed to identify proteins in B-AMEVs as the potential biomarkers for adenomyosis.

Materials and methods

Patients and samples. Adenomyotic lesions (n=31) were collected from patients with adenomyosis undergoing hysterectomy in the Department of Obstetrics and Gynecology of The First Affiliated Hospital of Chongqing Medical University (Chongqing, China). Plasma samples of patients with adenomyosis (n=25) and without adenomyosis (n=31, control) were collected from The Affiliated Hospital of Zunyi Medical University (Guizhou, China) during June 2018 to March 2021. The patients with adenomyosis or without adenomyosis were diagnosed by two gynecological pathologists via examining histologic sections of surgical specimens. The recruited women were premenopausal with regular menstrual cycles and at proliferative or secretory phase during the procedure. Any recruited women with indication of concomitant endometriosis, endometrial pathology or malignancy, history of hormone therapy or intrauterine device placement within 3 months preoperatively were all excluded. The plasma samples of patients with adenomyosis or without adenomyosis were collected before hysterectomy and recruited as the surgical specimens of uterus diagnosed by the gynaecological pathologist. The age distribution of tissue group of adenomyosis were between 44 to 50 years old, and blood sample of adenomyosis group were 36 to 53 years, and blood sample of control group were 37 to 49 years (Table I).

Magnetic resonance imaging (MRI). All patients underwent a pelvic enhanced MRI examination using a standardized protocol prior to sample collection (Magnetom symphony 1.5T MRI Tim system; Siemens Medical Solutions), in order to define the size, volume and location of the adenomyotic lesions following enhancement with gadolinium.

Haematoxylin and eosin (H&E) staining. All collected adenomyotic tissue samples were fixed in 10% neutral-buffered formalin overnight at room temperature, embedded in paraffin and cut into 5- μ m sections. Then, they were stained in hematoxylin for 10 min at room temperature and counterstained in 1% eosin solution for 4 min at room temperature using a previously reported method (9). The H&E staining slides were examined using a light microscope (BX51; Olympus Corporation).

Isolation of T-AMEVs and B-AMEVs from patients with adenomyosis. T-AMEVs and B-AMEVs were isolated and purified using a previously published protocol with some modifications (10,11). Freshly collected adenomyosis lesions were washed in 4°C cold PBS (HyClone; Cytiva) and immediately homogenized between two pieces of ground glass. The resulting cells were resuspended in 4°C cold PBS. The supernatants were centrifuged twice (800 x g for 10 min, then 1,000 x g for 10 min) at 4°C and ultrafiltered through a 1.2- μ m Minisart Syringe Filter (Sartorius AG) to remove cells and cell fragments.

Peripheral blood samples were collected into vacutainer tubes and centrifuged twice at 4°C, 2,000 x g for 10 min. The supernatant was ultrafiltered through a 1.2- μ m Minisart Syringe Filter (Sartorius AG) to remove cells and cell fragments. The filtrate was stored at -80°C until further differential centrifugation.

The resulting tissue or peripheral blood supernatant was subjected to differential centrifugation (50,000 x g for 90 min followed by 100,000 x g for 90 min) at 4°C. The precipitate was resuspended in 1 ml PBS. The retained precipitates were further purified by layering onto iodixanol density gradient medium (Axis-Shield Diagnostics) using a top-down gradient of 5, 10, 20, 30, 40 and 50% with centrifugation at 4°C, 100,000 x g for 90 min. The purified EVs were centrifuged at 4°C, 100,000 x g for 90 min, and the pellets were resuspended in 1 ml PBS, then stored at -80°C until further processing. The protein content of the purified EVs was quantified using an Enhanced BCA Protein Assay kit (Beyotime Institute of Biotechnology).

Transmission electron microscopy (TEM) with negative contrast staining. A 1- μ l sample of purified EVs was mixed with 100 μ l PBS solution, dried on a newly discharged 300-mesh Formvar/carbon-coated TEM grid (Ted Pella, Inc.) at room temperature, then negatively stained with 2% potassium phosphotungstate overnight at room temperature. All transmission electron micrographs were obtained using an H7500 transmission electron microscope (Hitachi, Ltd.) operating at 80 kV.

Low-vacuum scanning electron microscopy (LVSEM). Purified EVs (1 μ l) were resuspended in 100 μ l PBS, then in 900 μ l 2.5% glutaraldehyde solution (cat. no. P1126; Beijing Solarbio Science & Technology Co., Ltd.) at 4°C overnight. Micrographs of AMEVs were acquired using a low-vacuum scanning electron microscope (Nova Nano SEM 450; FEI; Thermo Fisher Scientific, Inc.) operated at 5 kV.

Nanoparticle tracking analysis (NTA). Purified EVs (1 μ l) were diluted in PBS (1 ml) and quantified using NTA (Nanosight NS 3000; Malvern Instruments, Ltd.) to determine the size distribution and particle concentration.

Liquid chromatography-mass spectrometry (LC-MS). LC-MS was performed according to a protocol described in a previous study with some modifications (12). In positive ionization mode, A Q-Exactive mass spectrometer (Thermo Fisher Scientific, Inc.) was used as the detector. Protein identification was performed with MASCOT software (version 2.3; Matrix

Table I. Characteristics of the patients with adenomyosis.

Characteristics	Adenomyotic lesion donors, n=31	Blood donors, n=25	P-value
Age, years	44.03±5.05	41.84±6.67	0.16
Uterine volume, cm ³	546.57±373.23	409.30±189.17	0.10
Age at menarche, years	13.45±1.29	13.96±1.27	0.15
Age at first marriage, years	22.71±2.37	22.40±2.55	0.64
Pregnancy	3.45±1.67	3.60±1.85	0.75
Parity	1.42±0.62	1.60±1.12	0.45
Dysmenorrhea, n (%)	21 (67.7)	19 (76.0)	0.42
Hypermenorrhea, n (%)	15 (48.3)	11 (44.0)	0.42

Science, Inc.) by searching the UniProt database (<https://www.uniprot.org/taxonomy/9606>). Carbamidomethylation of cysteines was set as a fixed modification. Trypsin was added at 1:50 trypsin:protein mass ratio for the first digestion overnight and a 1:100 trypsin:protein mass ratio for a second 4-h digestion. The maximal mass tolerance in MS mode was set to 20 ppm for the first search, and the fragment mass tolerance was set to 0.6 Da. The maximum false discovery rates (FDRs) for both peptide and protein identification were set to 0.05.

Gene ontology (GO) annotation and kyoto encyclopedia of genes and genomes (KEGG) pathway analysis. Functional enrichment analyses of the GO terms and KEGG pathways enriched in the proteins were conducted using the STRING database (version 11.0) (<https://string-db.org/>), with the entire human genome serving as the reference. GO analysis of enriched proteins was conducted for cellular component, molecular function and biological process annotation. The online Venn diagram tool FunRich3.1.3 (<http://funrich.org/download>) was used to compare T-AMEV and B-AMEV protein data with proteins in the Vesiclepedia database (12,13).

Western blot analysis. Protein expression was examined using previously published protocols with some modifications (14). In brief, total protein was extracted using Membrane and Cytosol Protein Extraction Kit (Beyotime Institute of Biotechnology) and protein concentration was determined using Enhanced BCA Protein Assay Kit (Beyotime Institute of Biotechnology) according to the manufacturer's instructions. Equal amounts of proteins (~30 µg per sample) were separated via 12% SDS-PAGE (Beyotime Institute of Biotechnology). The separated proteins were transferred to a 0.45-µm PVDF membrane (MilliporeSigma) and blocked in 0.5% bovine serum albumin solution for 30 min at 37°C, then incubated with anti-flotillin-2 (1:1,000; cat. no. ab181988; Abcam), anti-CD9 (1:2,000; cat. no. ab92726; Abcam), anti-CD63 (1:1,000; cat. no. ab134045; Abcam), anti-HSP90A (1:500; cat. no. AF5368; Affinity Biosciences), anti-STIP1 (1:1,000; cat. no. ab126724; Abcam), anti-TAGLN-2 (1:500; cat. no. AF12053; Affinity Biosciences) and anti-GAPDH (1:1,000; cat. no. E021060-03; EarthOx Life Sciences) antibodies at 4°C overnight. After three washes with wash buffer [PBS (pH 7.2; HyClone; Cytiva) + 0.1% Tween 20 (Beijing

Solarbio Science & Technology Co., Ltd.)], the membrane was incubated with a HRP-conjugated goat polyclonal secondary antibody against rabbit IgG-H&L (cat. no. E030130; EarthOx Life Sciences) for 1 h at 37°C. After washing with wash buffer, immunoreactive bands were visualized using ECL detection reagent (cat. no. WBKLS0050; MilliporeSigma). The films were scanned using an Azure c400 instrument (Azure Biosystems, Inc.), and the labelled bands were semi-quantified using ImageJ software (version 1.8.0; National Institutes of Health).

Statistical analysis. Data analysis was performed using SPSS software (version 21; IBM Corp.). Normally distributed data are expressed as the mean ± SD and were analysed using unpaired t-tests. The incidence of hypermenorrhoea and dysmenorrhea are presented as fractions and percentages and were statistically compared using χ^2 tests. $P < 0.05$ was considered to indicate a statistically significant difference.

Results

MRI and pathological characteristics of patients with adenomyosis. Patients with adenomyosis were diagnosed using MRI before hysterectomy and histopathological examination after hysterectomy. MRI indicated diffuse thickening of the myometrium, an irregular junctional zone and the presence of localized lesions in the posterior myometrium (Fig. 1A-C). H&E staining showed adenomyosis lesions in the posterior wall of the uterus (Fig. 1D and E).

Characterization of T-AMEVs and B-AMEVs. TEM, LVSEM and NTA were used to examine the morphology and size distribution of T-AMEVs and B-AMEVs. The TEM (Fig. 2A) and LVSEM (Fig. 2B) results suggested that the T-AMEVs and B-AMEVs had a lipid bilayer membrane and spherical shape. NTA showed that the average diameters of the T-AMEVs and B-AMEVs were 150.9±102.2 and 194.1±66.81 nm, respectively (Fig. 2C). Western blot analysis showed the presence of CD9, CD81 and flotillin-2 in both T-AMEVs and B-AMEVs (Fig. 2D).

Proteomic analysis of T-AMEVs and B-AMEVs. Mass spectrometric data for T-AMEVs and B-AMEVs were compared

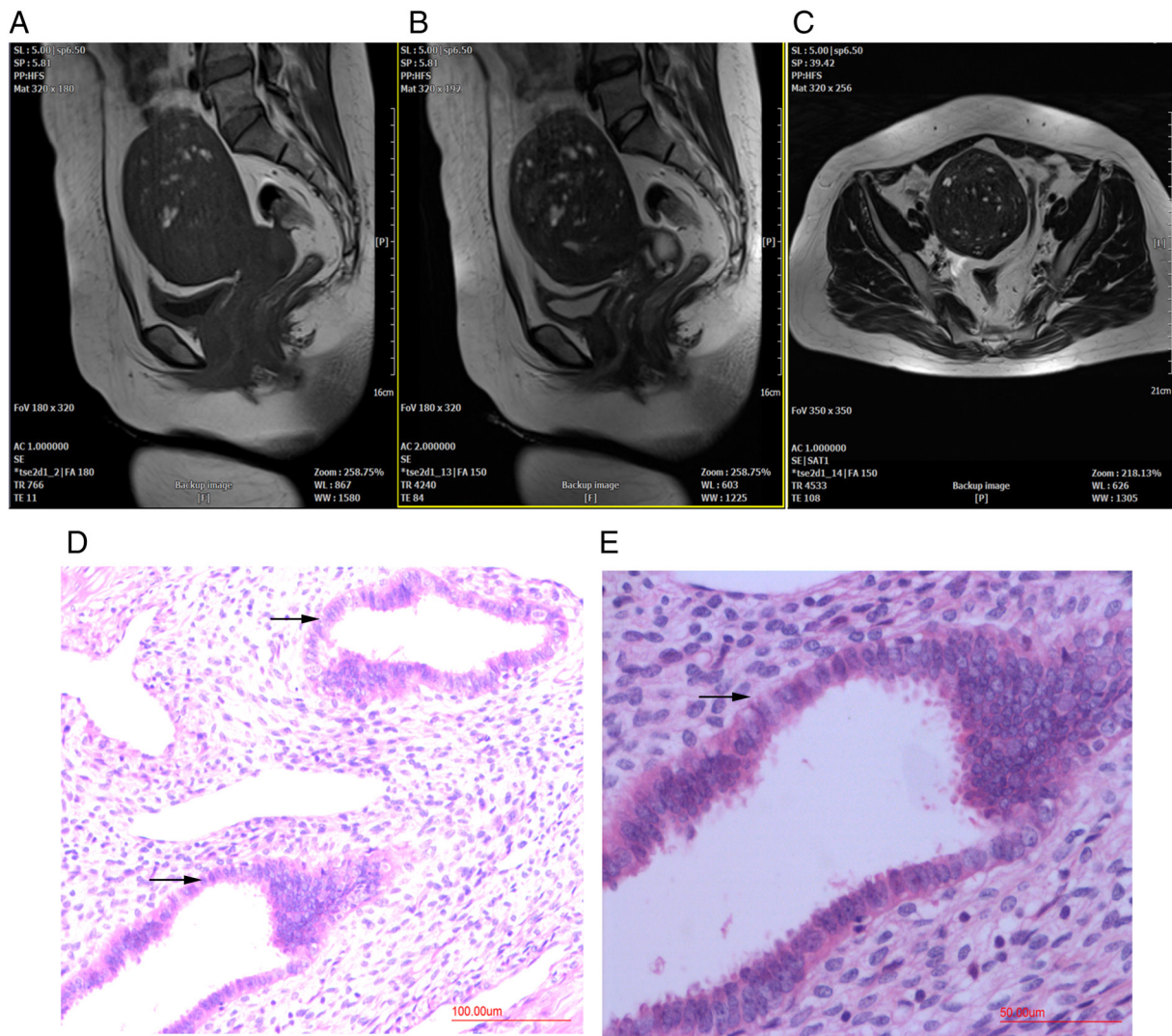


Figure 1. Magnetic resonance imaging and pathological diagnosis of patients with adenomyosis. (A) Sagittal T1-weighted image, (B) sagittal T2-weighted image and (C) coronal T2-weighted image of the uterus, showing diffuse thickening of the posterior myometrium of adenomyosis. Haematoxylin-eosin staining of an adenomyosis lesion (black arrows) at (D) magnification, x200 and (E) magnification, x400.

to the EV protein data from the Vesiclepedia database. A total of 2,195/2,573 proteins (85.30%) in T-AMEVs overlapped with entries in Vesiclepedia. For B-AMEVs, 313/406 proteins (77.09%) overlapped with Vesiclepedia (Fig. 3A). A total of 211 proteins were simultaneously expressed in T-AMEVs and B-AMEVs (Table SI), including 205 proteins that overlapped with entries in Vesiclepedia and 6 proteins that were not in Vesiclepedia (Fig. 3A).

Further study of the proteomic data revealed that 15 proteins in T-AMEVs were related to the EMT process: Moesin, ezrin, glycogen synthase kinase-3 β , 78-kDa glucose-regulated protein, C-terminal-binding protein 1, C-terminal-binding protein 2, cell cycle and apoptosis regulator protein 2, interleukin-like EMT inducer, histidine triad nucleotide-binding protein 1 (HINT1), stimulator of interferon genes protein, FK506-binding protein 1A, junctional adhesion molecule 1, ubiquitin A-52 residue ribosomal protein fusion product 1 (UBA52), melanoma differentiation-associated protein 9 and transforming protein RhoA (UniProt database) (Table SII). Similarly, 3 proteins in B-AMEVs were related to the EMT process: large tumour suppressor homolog 2,

HINT1, and UBA52. Among the EMT-related proteins, HINT1 and UBA52 were simultaneously expressed in T-AMEVs and B-AMEVs (Fig. 3B; Table SIII), which also overlapped with the Vesiclepedia database (Fig. 3B).

A total of 63 proteins in T-AMEVs and 9 proteins in B-AMEVs were found to promote the invasion of target cells in adenomyosis (15). Of these, 6 proteins were shared between T-AMEVs and B-AMEVs and overlapped with entries in Vesiclepedia: Fibulin-1, protein S100-A9, plasminogen, fascin, heat shock cognate 71-kDa protein and Rho GDP-dissociation inhibitor 1 (Fig. 3C; Table SIV).

GO and KEGG pathway analysis of proteins simultaneously expressed in T-AMEVs and B-AMEVs. GO and KEGG pathway analyses of the proteins simultaneously expressed in T-AMEVs and B-AMEVs were performed using the STRING database. The biological processes of the 211 proteins primarily referred to the terms 'regulation of actin cytoskeleton organization', 'regulation of oxidative stress-induced cell death' and 'regulation of cell morphogenesis' (Fig. S1A). The cellular components of the 211 proteins were primarily related to the

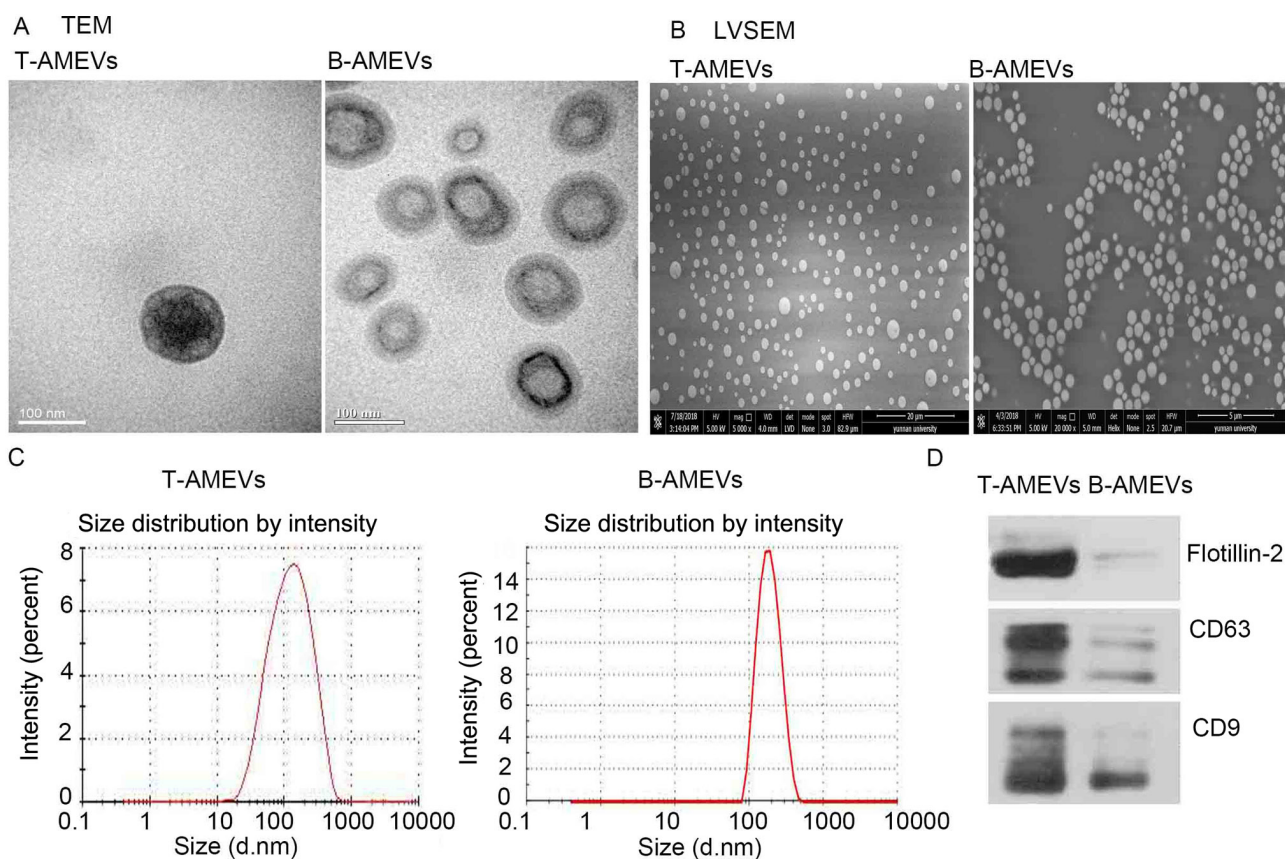


Figure 2. Characterization of T-AMEVs and B-AMEVs. (A) TEM and (B) LVSEM images of T-AMEVs and B-AMEVs. (C) The size distributions of T-AMEVs and B-AMEVs were evaluated using nanoparticle tracking analysis. The expression of CD9, CD63 and flotillin-2 in T-AMEVs and B-AMEVs was detected by western blotting (D). T-AMEV, tissue adenomyosis-derived extracellular vesicle; B-AMEV, blood adenomyosis-derived extracellular vesicle; TEM, Transmission electron microscopy; LVSEM, low-vacuum scanning electron microscopy; d, diameter; nm, nanometre.

terms ‘cortical cytoskeleton’, ‘cortical actin cytoskeleton’, ‘actin cytoskeleton’ and ‘intrinsic component of the cytoplasmic side of the plasma membrane’ (Fig. S1B). The molecular functions of the 211 proteins were primarily enriched in the terms ‘actin filament binding’, ‘protein-containing complex binding’, ‘cytoskeletal protein binding’, ‘actin binding’ and ‘structural constituent of cytoskeleton’ (Fig. S1C).

KEGG pathway analysis revealed that the enriched pathway terms of the 211 proteins with FDRs <0.05 were the ‘hypoxia-inducible factor (HIF)-1 signalling pathway’, ‘metabolic pathways’, ‘central carbon metabolism in cancer’, ‘peroxisome proliferator-activated receptor (PPAR) signalling pathway’ and ‘autophagy’ (Table SV). Among these enriched pathways, the ‘PPAR signalling pathway’, ‘HIF-1 signalling pathway’ and ‘autophagy’ are related to the proliferation, metastasis and autophagy of endometrial cells (Table SV).

HSP90A, *STIP1* and *TAGLN-2* in T-AMEVs and B-AMEVs were identified as potential biomarkers for adenomyosis. It has previously been suggested that *STIP1* is upregulated in women with adenomyosis compared with those without adenomyosis (16). In the present study, analysis in the STRING database showed that *STIP1* and *HSP90A* acted synergistically (17) (Fig. 4A). *TAGLN-2* is a homolog of transgelin, which is an early marker of smooth muscle cell differentiation (18), and STRING database analysis showed that *TAGLN-2* and *TAGLN-3* act synergistically (Fig. 4B).

Furthermore, 3 out of 211 proteins shared between T-AMEVs and B-AMEVs, (*HSP90A*, *STIP1* and *TAGLN-2*) were chosen as potential biomarkers for adenomyosis. Research has reported that *STIP1* is over-expressed in adenomyosis. *STIP1* is one of the co-chaperone proteins that form the structural parts of the HSP90 machinery (16). *TAGLN-2* is a homolog of transgelin, which is an early marker of smooth muscle cell differentiation (18). In adenomyosis, myocytes exhibit cellular hypertrophy and show differences in cytoplasmic organelles, nuclear structures and intercellular junctions with normal myometrium (1). Therefore, the present study selected the three proteins as potential biomarkers for adenomyosis. FunRich3.1.3 software analysis demonstrated that these three proteins overlapped with entries in the Vesiclepedia database, indicating that they are EV-derived proteins (Fig. 4C).

To further determine whether *HSP90A*, *STIP1* and *TAGLN-2* were expressed only in AMEVs and could be detected in EV samples, plasma EVs were collected from women without adenomyosis/endometriosis (n=31) as a control group (Table SVI; Fig. S2). Western blot analysis revealed that *HSP90A*, *STIP1* and *TAGLN-2* were detectable in both T-AMEVs and B-AMEVs, but not in EVs of the control group (Fig. 4D and E). *STIP1* bands were detected at ~63 kDa (predicted molecular weight, 63 kDa). Semi-quantitative analysis showed that *STIP1* was expressed in B-AMEVs and T-AMEVs. LC-MS showed that the exponentially modified

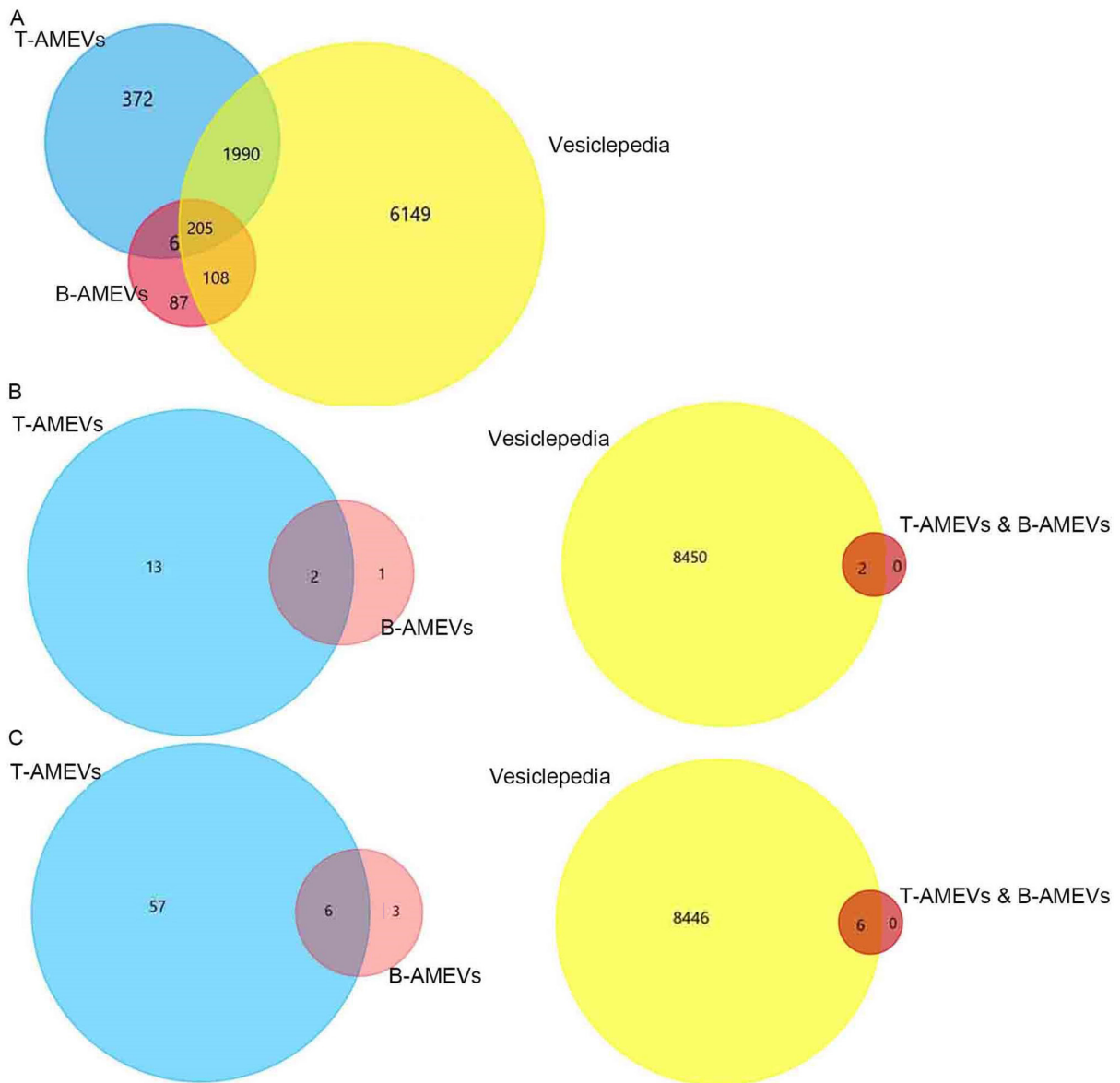


Figure 3. Proteomic characteristics of T-AMEVs and B-AMEVs. (A) Venn diagram of proteins in T-AMEVs and B-AMEVs overlapping with proteins in the Vesiclepedia database. (B) EMT-associated and (C) invasion-associated proteins in T-AMEVs and B-AMEVs. The proteins overlapping between T-AMEVs and B-AMEVs were also found in Vesiclepedia (right panels). T-AMEV, tissue adenomyosis-derived extracellular vesicle; B-AMEV, blood adenomyosis-derived extracellular vesicle.

protein abundance index of STIP1 in T-AMEVs and B-AMEVs was 0.58 and 0.11, respectively.

Discussion

Adenomyosis is a disease associated with endometrial invasion. However, the factors involved in the invasive capacity of the endometrium remain to be further studied. EVs are a new type of intercellular communication mode. Our previous study demonstrated EVs play an important role in modulating the disease process of adenomyosis (7). Therefore, it is hypothesized that it is necessary to investigate EVs in the diagnosis and pathogenesis of adenomyosis. EVs have been isolated from the serum of patients with endometriosis (8). Therefore, it is important to investigate the role of EVs in the diagnosis and pathogenesis of adenomyosis.

In the present study, EVs were first extracted from lesion homogenates and peripheral blood of patients with adenomyosis. The protein cargoes of AMEVs were analysed using LC-MS, and potential biomarkers for adenomyosis were identified by proteomic analysis. The proteomic results showed that 211 vesicular proteins were simultaneously expressed in T-AMEVs and B-AMEVs. Among the 211 proteins, 2 were associated with EMT, and 6 with invasion. The present results are consistent with previously reported results that EMT (19,20) and the invasiveness (21) of endometrial cells play critical roles in the pathogenesis and development of adenomyosis. The 211 cargo proteins simultaneously expressed in T-AMEVs and B-AMEVs might represent the molecular characteristics of adenomyosis.

GO analysis revealed that proteins in T-AMEVs and B-AMEVs were enriched in the 'regulation of cellular

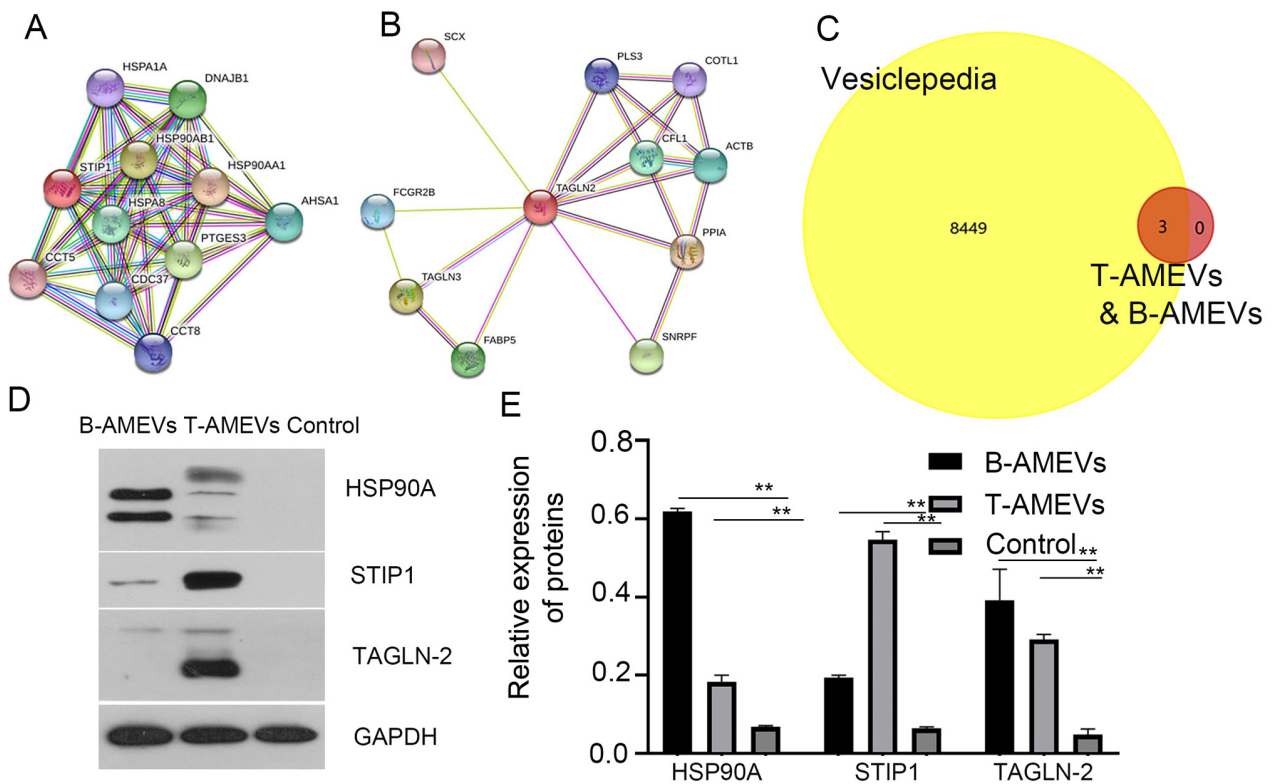


Figure 4. HSP90A, STIP1 and TAGLN-2 are expressed in B-AMEVs and T-AMEVs. (A) Protein-protein interaction network of STIP1 and HSP90A and (B) TAGLN-2 and TAGLN-3 as revealed by STRING database analysis. (C) Venn diagrams of proteins simultaneously expressed in T-AMEVs and B-AMEVs against the database of Vesiclepedia. (D and E) HSP90A, STIP1 and TAGLN-2 were present in T-AMEVs and B-AMEVs from patients with adenomyosis, but not in those of patients in the control group. ** $P \leq 0.01$. T-AMEV, tissue adenomyosis-derived extracellular vesicle; B-AMEV, blood adenomyosis-derived extracellular vesicle; HSP90A, heat shock protein 90 α , STIP1, stress-induced phosphoprotein 1; TAGLN-2, transgelin 2.

component organization', 'regulation of cytoskeleton organization' and 'regulation of cell morphogenesis', indicating that the cargos of T-AMEVs and B-AMEVs are closely related to EMT. This regulatory characteristic indicated endometrial cells had a trend toward EMT (Fig. S1A). The enrichment of 'cytoplasmic part' and 'cortical cytoskeleton' terms in the GO cellular component analysis reflects the EV origin (Fig. S1B). In addition, the terms 'cytoplasmic vesicle lumen' and 'secretory granule lumen' indicate that EV may originate from the cytoplasmic vesicle lumen and the secretory granule lumens (Fig. S1B). 'Cytoskeletal protein binding', 'actin filament binding' and 'structural constituent of cytoskeleton' were the most enriched molecular function terms, which suggests that direct regulation of the cytoskeleton might be the primary regulatory function of T-AMEVs and B-AMEVs (Fig. S1C).

KEGG pathway analysis revealed that the 211 proteins of T-AMEVs and B-AMEVs are involved in several signalling pathways, including 'carbon metabolism', 'glycolysis' and the 'biosynthesis of amino acids' (Table SV), which indicates that T-AMEVs and B-AMEVs had the capacity to transfer information to other cells and thereby influence the recipient cell function (5). Additionally, some proteins were enriched in the HIF-1 signalling pathways, which are related to the metastatic and proangiogenic capacity of adenomyotic endometrial cells (22), and in the PPAR signalling pathway, which is related to the proliferative capacity of adenomyotic endometrial cells (23). These results demonstrated that T-AMEVs

and B-AMEVs carry specific proteins that represent the pathological condition of adenomyosis and that these proteins are candidate biological biomarkers for adenomyosis.

Currently, there is no specific diagnostic biomarker for adenomyosis. The current non-invasive methods for the diagnosis of adenomyosis are transvaginal ultrasound or MRI (2). EVs are increasingly important as biomarkers for diseases (24). EVs are nanoscale lipid bilayer particles that contain nucleic acid and protein cargoes and can be secreted from cells under a variety of normal and pathological conditions. EVs have recently attracted widespread research interest due to their potential use as circulating biomarkers for a variety of diseases, including numerous types of cancers. EVs play a specific role in cancer pathogenesis and exhibit potential for use in non-invasive disease diagnosis and/or monitoring (25).

The presence of tumour-derived EVs in circulating body fluids means that EVs represent a readily available source of biomarkers. This observation suggests that EVs may have unique uses in longitudinal disease monitoring and the early detection of relapse (26). In addition, certain EV-related proteins and nucleic acid species have been reported to predict the response to treatment. Overall, accumulating evidence indicates that EVs are a rich and easily accessible source of cancer biomarkers.

From the 211 proteins simultaneously expressed in T-AMEVs and B-AMEVs, we aimed to identify proteins as potential EV-based biomarkers for adenomyosis. *In vitro*

experiments showed that patients with adenomyosis had significantly higher preoperative serum STIP1 levels than women without adenomyosis. Specifically, one study showed a positive correlation between STIP1 levels and adenomyosis (16). STIP1 is an adaptor protein that coordinates the functions of HSP70 and HSP90 in protein folding. Increased STIP1 expression is related to the pathogenesis of gynaecological malignancies, including ovarian cancer and endometrial cancer (16). Evidence suggests that STIP1 can stimulate DNA synthesis and enhance cell proliferation. Knockdown of STIP1 expression in cancer cells has been shown to reduce tumour invasiveness by downregulation of matrix metalloproteinases (MMPs) (27). Through STRING database analysis, we confirmed that STIP1 acts synergistically with HSP90A.

HSP90 proteins are highly conserved molecules that promote protein folding and block the aggregation of neosynthesized or incorrectly folded proteins. HSP90 has been detected in exosomes secreted from human cancer cells and is important in cancer development because it regulates tumour growth, adhesion, invasion, metastasis, angiogenesis, and apoptosis (28,29). HSP90 is overexpressed in a variety of cancers, including pancreatic, ovarian, breast, lung and endometrial cancers, oropharyngeal squamous cell carcinoma (SCC), and multiple myeloma. The high expression of HSP90 is considered a marker of poor prognosis in lung cancer, oesophageal cancer, bladder cancer, melanoma, and leukaemia (29). HSP90A is the inducible form of HSP90.

In addition, studies have indicated ultrastructural differences between smooth muscle cells from adenomyotic and normal myometria (1). TAGLN-2 is a homolog of transgelin, which is an early marker of smooth muscle cell differentiation (18), and its biological function involves the regulation of actin cytoskeleton dynamics by stabilizing actin fibres. Transgelin also participates in processes involving actin cytoskeleton remodelling, such as cell proliferation, differentiation, migration, and apoptosis. TAGLN-2 is also considered to be correlated with tumorigenesis, tumour metastasis and invasion, and it is highly expressed in uterine cervical SCC tissues and endometrial cancer (30). TAGLN-2 and TAGLN-3 work synergistically.

In our previous study, EVs isolated from adenomyotic tissue sample highly expressed STIP1, HSP90A and TAGLN2 (7). To further determine whether HSP90A, STIP1 and TAGLN-2 were expressed only in AMEV and can be detected in EV samples, plasmaEVs were isolated from women without adenomyosis/ endometriosis, and western blotting was used to measure the protein expression levels of STIP1, HSP90A and TAGLN-2 in T-AMEVs, B-AMEVs and serum EVs. The results suggested that STIP1, HSP90A and TAGLN-2 were expressed in T-AMEVs and B-AMEVs but not in EVs of control group. This result further supports the use of STIP1, HSP90A and TAGLN-2 as biomarkers for adenomyosis.

In conclusion, cargo proteins contained in EVs derived from adenomyotic tissue and the peripheral blood of patients with adenomyosis may induce endometrial cell invasion and EMT. High expression of STIP1, HSP90A and TAGLN-2 may relate to endometrial cell growth, invasion, EMT and smooth muscle cell differentiation. The present study is limited by the sample size of clinical patients. Therefore, further studies should increase the volume of single blood samples by increasing EV output to facilitate LC-MS detection of EV

proteins in the blood of a single patient, and further studies should be performed to verify the three proteins' function in pathophysiology of adenomyosis using experimental assays. STIP1, HSP90A and TAGLN-2 were expressed in EVs derived from adenomyotic tissue and the peripheral blood of patients with adenomyosis. These proteins could represent potential biomarkers for the clinical diagnosis of adenomyosis.

Acknowledgements

Not applicable.

Funding

This work was partially supported by The Chongqing Basic Science and Frontier Technology Research Project (grant no. cstc2017jcyjAX0432).

Availability of data and materials

The datasets used and/or analysed during the current study are available from the corresponding author on reasonable request.

Authors' contributions

ZW, LF, BY and DC conceived and designed the study and analysed and interpreted the data. DC performed the experiments and acquired the data with the assistance of LZ, HQ and YW for *in vitro* work. DC, LZ and YX analysed the data and were involved in drafting the manuscript. DC, BY and LF wrote and revised the paper critically. All of the other authors were involved in writing the manuscript. DC collected the blood and tissue samples from adenomyosis patients. All authors read and approved the final manuscript. LF and ZW confirm the authenticity of all the raw data.

Ethics approval and consent to participate

The study protocol for human samples was approved by the Ethics Committee of Chongqing Medical University (approval no. 2018014) and the Affiliated Hospital of Zunyi Medical University (Guizhou, China; approval no. 20211-005). The study was carried out in accordance with the Declaration of Helsinki Declaration of the World Medical Association. All patients (including the control group) provided written informed consent.

Patient consent for publication

Not applicable.

Competing interests

The authors declare that they have no competing interests.

References

1. Benagiano G, Habiba M and Brosens I: The pathophysiology of uterine adenomyosis: An update. *Fertil Steril* 98: 572-579, 2012.

2. Xu R, Greening DW, Zhu HJ, Takahashi N and Simpson RJ: Extracellular vesicle isolation and characterization: Toward clinical application. *J Clin Invest* 126: 1152-1162, 2016.
3. Colombo M, Raposo G and Théry C: Biogenesis, secretion, and intercellular interactions of exosomes and other extracellular vesicles. *Annu Rev Cell Dev Biol* 30: 255-289, 2014.
4. Henderson MC and Azorsa DO: The genomic and proteomic content of cancer cell-derived exosomes. *Front Oncol* 2: 38, 2012.
5. Yáñez-Mó M, Siljander PR, Andreu Z, Zavec AB, Borràs FE, Buzas EI, Buzas K, Casal E, Cappello F, Carvalho J, *et al*: Biological properties of extracellular vesicles and their physiological functions. *J Extracell Vesicles* 4: 27066, 2015.
6. Momen-Heravi F, Getting SJ and Moschos SA: Extracellular vesicles and their nucleic acids for biomarker discovery. *Pharmacol Ther* 192: 170-187, 2018.
7. Chen D, Qiao H, Wang Y, Zhou L, Yin N, Fang L and Wang Z: Adenomyosis-derived extracellular vesicles endow endometrial epithelial cells with an invasive phenotype through epithelial-mesenchymal transition. *Genes Dis* 7: 636-648, 2020.
8. Qiu JJ, Lin XJ, Zheng TT, Tang XY, Zhang Y and Hua KQ: The exosomal long noncoding RNA aHIF is upregulated in serum from patients with endometriosis and promotes angiogenesis in endometriosis. *Reprod Sci* 26: 1590-1602, 2019.
9. Roeder HA, Cramer SF and Leppert PC: A look at uterine wound healing through a histopathological study of uterine scars. *Reprod Sci* 19: 463-473, 2012.
10. Wang GJ, Liu Y, Qin A, Shah SV, Deng ZB, Xiang X, Cheng Z, Liu C, Wang J, Zhang L, *et al*: Thymus exosomes-like particles induce regulatory T cells. *J Immunol* 181: 5242-5248, 2008.
11. Coumans FAW, Brisson AR, Buzas EI, Dignat-George F, Drees EEE, El-Andaloussi S, Emanuelli C, Gasecka A, Hendrix A, Hill AF, *et al*: Methodological guidelines to study extracellular vesicles. *Circ Res* 120: 1632-1648, 2017.
12. Pathan M, Keerthikumar S, Chisanga D, Alessandro R, Ang CS, Askenase P, Batagov AO, Benito-Martin A, Camussi G, Clayton A, *et al*: A novel community driven software for functional enrichment analysis of extracellular vesicles data. *J Extracell Vesicles* 6: 1321455, 2017.
13. Pathan M, Keerthikumar S, Ang CS, Gangoda L, Quek CMJ, Williamson NJ, Mouradov D, Sieber OM, Simpson RJ, Salim A, *et al*: FunRich: A standalone tool for functional enrichment analysis. *Proteomics* 15: 2597-2601, 2015.
14. Wang DJ, Wang CM, Wang YT, Qiao H, Fang LQ and Wang ZB: Lactation-related MicroRNA expression in microvesicles of human umbilical cord blood. *Med Sci Monit* 22: 4542-4554, 2016.
15. Morgat A, Lombardot T, Coudert E, Axelsen K, Neto TB, Gehant S, Bansal P, Bolleman J, Gasteiger E, de Castro E, *et al*: Enzyme annotation in UniProtKB using Rhea. *Bioinformatics* 36: 1896-1901, 2020.
16. Wang HS, Tsai CL, Chang PY, Chao A, Wu RC, Chen SH, Wang CJ, Yen CF, Lee YS and Wang TH: Positive associations between upregulated levels of stress-induced phosphoprotein 1 and matrix metalloproteinase-9 in endometriosis/adenomyosis. *PLoS One* 13: e0190573, 2018.
17. Tsai CL, Lee YS, Chao A, Yen CF, Wang HS and Wang TH: Associations between a single nucleotide polymorphism of stress-induced phosphoprotein 1 and endometriosis/adenomyosis. *Taiwan J Obstet Gynecol* 57: 270-275, 2018.
18. Li L, Miano JM, Cserjesi P and Olson EN: SM22 alpha, a marker of adult smooth muscle, is expressed in multiple myogenic lineages during embryogenesis. *Circ Res* 78: 188-195, 1996.
19. Benagiano G, Brosens I and Habiba M: Structural and molecular features of the endomyometrium in endometriosis and adenomyosis. *Hum Reprod Update* 20: 386-402, 2014.
20. Syn N, Wang L, Sethi G, Thiery JP and Goh BC: Exosome-mediated metastasis: From epithelial-mesenchymal transition to escape from immunosurveillance. *Trends Pharmacol Sci* 37: 606-617, 2016.
21. Gaetje R, Kotzian S, Herrmann G, Baumann R and Starzinski-Powitz A: Invasiveness of endometriotic cells in vitro. *Lancet* 346: 1463-1464, 1995.
22. Zhou S, Yi T, Liu R, Bian C, Qi X, He X, Wang K, Li J, Zhao X, Huang C and Wei Y: Proteomics identification of annexin A2 as a key mediator in the metastasis and proangiogenesis of endometrial cells in human adenomyosis. *Mol Cell Proteomics* 11: M112.017988, 2012.
23. Wu Y and Guo SW: Peroxisome proliferator-activated receptor-gamma and retinoid X receptor agonists synergistically suppress proliferation of immortalized endometrial stromal cells. *Fertil Steril* 91 (Suppl 5): S2142-S2147, 2009.
24. Taleb RSZ, Moez P, Younan D, Eisenacher M, Tenbusch M, Sitek B and Bracht T: Protein biomarker discovery using human blood plasma microparticles. *Methods Mol Biol* 1959: 51-64, 2019.
25. Lane RE, Korbie D, Hill MM and Trau M: Extracellular vesicles as circulating cancer biomarkers: Opportunities and challenges. *Clin Trans Med* 7: 14, 2018.
26. Hornick NI, Huan J, Doron B, Goloviznina NA, Lapidus J, Chang BH and Kurre P: Serum exosome microRNA as a minimally-invasive early biomarker of AML. *Sci Rep* 5: 11295, 2015.
27. Walsh N, Larkin A, Swan N, Conlon K, Dowling P, McDermott R and Clynes M: RNAi knockdown of Hop (Hsp70/Hsp90 organising protein) decreases invasion via MMP-2 down regulation. *Cancer Lett* 306: 180-189, 2011.
28. Sims JD, McCready J and Jay DG: Extracellular heat shock protein (Hsp)70 and Hsp90 α assist in matrix metalloproteinase-2 activation and breast cancer cell migration and invasion. *PLoS One* 6: e18848, 2011.
29. Wu J, Liu T, Rios Z, Mei Q, Lin X and Cao S: Heat shock proteins and cancer. *Trends Pharmacol Sci* 38: 226-256, 2017.
30. Meng T, Liu L, Hao R, Chen S and Dong Y: Transgelin-2: A potential oncogenic factor. *Tumour Biol* 39: 1010428317702650, 2017.



This work is licensed under a Creative Commons Attribution-NonCommercial-NoDerivatives 4.0 International (CC BY-NC-ND 4.0) License.